Rheological Behavior and Mechanical Properties of High-Density Polyethylene Blends with Different Molecular Weights

Lu Bai, Yan-Mei Li, Wei Yang, Ming-Bo Yang

College of Polymer Science and Engineering, State Key Laboratory of Polymer Materials Engineering, Sichuan University, Chengdu, 610065, Sichuan, People's Republic of China

Received 4 May 2009; accepted 24 February 2010
DOI 10.1002/app.32329
Published online 3 June 2010 in Wiley InterScience (www.interscience.wiley.com).

ABSTRACT: The dynamic rheological and mechanical properties of the binary blends of two conventional high-density polyethylenes [HDPEs; low molecular weight (LMW) and high molecular weight (HMW)] with distinct different weight-average molecular weights were studied. The rheological results show that the rheological behavior of the blends departed from classical linear viscoelastic theory because of the polydispersity of the HDPEs that we used. Plots of the logarithm of the zero shear viscosity fitted by the Cross model versus the blend composition, Cole–Cole plots, Han curves, and master curves of the storage and loss moduli indicated the LMW/HMW blends of different compositions were miscible in the melt state. The tensile yield strength of the blends generally followed the linear additivity rule, whereas the elongation at break and impact strength were lower than those predicted by linear additivity; this suggested the incompatibility of the blends in solid state. © 2010 Wiley Periodicals, Inc. J Appl Polym Sci 118: 1356–1363, 2010

Key words: mechanical properties; miscibility; weight average molecular weight; polyethylene (PE); rheology

INTRODUCTION

Polyethylene (PE), one of the most widely used general plastics, has drawn much attention from both industrial engineers and academic researchers. To improve processing performance and achieve tailored properties, PE blends have been widely used.[1–7] Blending is a common practice in the polyolefin area. However, the enhancement of the processing performance and the properties of PE blends is controlled by the phase morphology of the blends in the melt and in the final solid state.

To date, many studies have been done on the phase behavior of PE blends. Molecular parameters, such as weight-average molecular weight (M_w), molecular weight distribution, branch content (BC), branch type, and composition distribution, have been found to strongly influence the miscibility of PE blends. Some basic disagreements, even contradictory results, concerning the miscibility of PE blends can be found in the literature where different techniques were used.[8–20] Hill and coworkers[11–17] pointed out that liquid–liquid phase separation (LLPS) could take place in many PE blends; however, Wignal and coworkers[18,19] did not agree with this opinion. By using techniques including differential scanning calorimetry (DSC) and transmission electron spectroscopy to investigate the quenched phase morphology, Hill's group[11–17] reported the LLPS phenomena in PE blends. However, Wignal and coworkers[18,19] considered that studies in the solid state do not necessarily reflect the structure of the melt and raised an objection by using small-angle neutron scattering. However, they did not deny the LLPS in the PE blends and figured that LLPS could be observed under some conditions. Tanem and Stori[20] reported the strong influence of M_w on the phase behavior of a linear low-density polyethylene (LLDPE)/linear polyethylene (LPE) blend. He found that the extent of phase separation increased when the molecular weight of the linear blend component was increased.

Despite decades of study, researchers still cannot agree with each other on the miscibility of PE blends. Because of the limit of the techniques, Hill and Barham[21] pointed out that if there was any LLPS in LPE/LPE blends taking place as a result of molecular weight differences, it could not be detected by traditional methods. Now, dynamic

Correspondence to: M.-B. Yang (yangmb@scu.edu.cn).
Contract grant sponsor: National Natural Science Foundation of China; contract grant number: 20734005.
Contract grant sponsor: Program for New Century Excellent Talents in University; contract grant number: NCET-08-382.
Contract grant sponsor: Special Funds for Major Basic Research of China; contract grant number: 2005CB623808.

© 2010 Wiley Periodicals, Inc.

rheological testing has been paid more and more attention because the rheological properties of polymers are sensitive to both the molecular structures and phase behaviors. Utracki[22] pointed out that if the strain amplitude was sufficiently small, dynamic rheological measurement would be the optimal method to obtain the phase behavior of blends.

The influence of the molecular parameters on the miscibility of LLDPE/low-density polyethylene (LDPE) blends and LLDPE/high-density polyethylene (HDPE) blends were extensively studied by Hussein, Williams, and coworkers[23–32] using rheological techniques. The M_w of LLDPE was observed to have a strong influence on its miscibility with LDPE.[26,30] Low-M_w metallocene-catalyzed linear low-density polyethylene (m-LLDPE) blends with LDPE were miscible at all compositions, whereas the blends of high-M_w m-LLDPE and LDPE showed partial miscibility at high LLDPE contents and immiscibility at low LLDPE contents with the same LDPE.[27] Similar results were found for different molecular weight Ziegler–Natta-catalyzed linear low-density polyethylene (ZN-LLDPE) blends with LDPE.[30] It was also found that the BC of m-LLDPE had an obvious effect on its miscibility with LDPE. With increased BC, m-LLDPE enhanced its miscibility with LDPE compared to a low-BC m-LLDPE.[28,31] However, the influence of BC on the miscibility of ZN-LLDPE/LDPE blends was different when a LDPE of high BC was used. Furthermore, the effect of the comonomer type of LLDPE on its miscibility with LDPE was also studied.[25,30] Fang et al.[33] also investigated the melt miscibility of m-LLDPE/LDPE, and an improved miscibility was reported to be promoted with increasing length of the short-chain branch in m-LLDPE.

The melt rheology of m-LLDPE blends with HDPE also revealed the strong influence of M_w on the melt miscibility at both high and low branching levels. Low-M_w m-LLDPE/HDPE blends were observed to be miscible at all compositions, whereas the viscosity of high-M_w m-LLDPE/HDPE blends showed negative deviation from the logarithm of additivity; this suggested a layered morphology for these blends.[32]

For binary blends of HDPE, LLDPE, and LDPE, it was reported that in the solid state, the LLDPE/LDPE and HDPE/LDPE blends were not miscible, but the LLDPE/HDPE blend was miscible,[34] and they were all miscible in the melt state.[7] The m-LLDPE/HDPE blend was also found to be miscible by rheological and morphological investigations.[35]

Blends of various PEs are commonplace, in particular, mixtures of LPE with branched polyethylene (BPE). The phase behavior of LPE/BPE blends has been studied intensively by the study of the rheological properties, and phase separations in blends of LPE and BPE have focused on components different in molecular parameters. However, less attention has been paid to the rheological performances and mechanical properties of HDPE blends (LPE/LPE) with different M_w values, although some opposite opinions have been presented.[36,37] Munoz-Escalona et al.[36] presented the dynamic viscoelasticity values of a series of blends of low-molecular-weight (LMW) and high-molecular-weight (HMW) m-HDPE. A single correlation between the storage modulus (G') and loss modulus (G'') showed that microphases did not exist in the melt for any composition, which was confirmed by dimensional stability measurements, which showed no deviation in the compositional variation of shrinkage values, a characteristic feature of miscible systems. However, Krishnaswamy and Yang[37] attributed the phase segregation of PE blends to the considerable differences in the molecular weight and melt viscosity.

In our previous study on the effect of M_w on the rheological properties for HDPE and its blends, no LLPS was found in the HDPE blends.[38] In this study, two linear PEs with distinctly different M_w's were chosen and melt-blended at different compositions; this was followed by investigation of the melt dynamic rheological properties and mechanical properties.

EXPERIMENTAL

Materials and sample preparation

Two different HDPEs, with the trademarks 2911 (Fushun, PR China) and 5000S (Lanzhou, PR China), designated as LMW and HMW, were supplied as pellets by Sinopec. The molecular parameters of materials, the M_w and polydispersity index [weight-average molecular weight/number-average molecular weight (M_w/M_n)] values obtained from GPC tests, and the density and comonomer content provided by the producer are listed in Table I.

The LMW/HMW blends were melt-blended in an SHJ-220 corotating twin-screw extruder (Nanjing Giant Co., Nanjing, PR China) with a length-to-diameter ratio of 32 with compositions (weight percentages) of 100/0, 90/10, 70/30, 50/50, 30/70, 10/90, and 0/100; these compositions were named LMW, LH10, LH30, LH50 LH70, LH90, and HMW in this study. The temperature profile used for blending was 190, 215, 225, and 215°C for the feed zone, compression zone, metering zone, and die end, respectively. The extruded threads were then pelletized. The pellets were dried at 80°C for 3 h and then injection-molded into rectangular bars and dumbbell-shaped specimens with a PS40E5ASE injection-molding machine (Nisseijushi Co., Japan) with a temperature profile of 195, 215, 230, and 210°C from the hopper to the nozzle. The extruded pellets were also compress-molded into desired disks at 180°C

TABLE I
Molecular Characteristics of the LMW/HMW Blends

Sample	Density (g/cm^3)	Comonomer content (mol %)	M_w ($\times 10^5$ g/mol)	M_n ($\times 10^4$ g/mol)	M_w/M_n	η^0 (Pa s)
LMW	0.96	Homopolymer	1.27	2.87	4.4	518
LH10	–	–	1.46	–	–	801
LH30	–	–	1.84	–	–	2,046
LH50	–	–	2.22	–	–	3,641
LH70	–	–	2.60	–	–	6,586
LH90	–	–	2.98	–	–	10,395
HMW	0.953	0.1 (propylene)	3.17	5.88	5.4	14,369

for the melt rheological measurements. Before the preparation of the blends, the polymers were stabilized by the addition of 0.3 wt % antioxidant to prevent thermooxidative degradation during processing.

GPC characterization

A model PL-GPC 220 UK (Polymer Laboratories Ltd., Shropshire, United Kingdom) instrument was used to characterize the molecular characteristics of the HDPEs. It was operated at 160°C with 1,2,4-trichlorobenzene (TCB) as a solvent. Four columns with pore sizes of 10^3, 10^4, 10^5, and 10^6 Å were calibrated with narrow-molecular-weight-distribution polystyrene samples. The columns were calibrated at 140°C with 0.1% polystyrene in TCB.[39]

Dynamic rheological measurements

Dynamic rheological measurements were carried out in a Bohlin Gemini 200 (Malvern Instruments, Ltd., Worcestershirem, United Kingdom) constant-strain rheometer with parallel-plate geometry. The diameter of the plate was 25 mm, and the gap was about 1 mm. All of the samples were tested at 140, 160, 180, and 200°C, respectively, and the frequency range adopted was 0.01–100 Hz. To keep the response in the viscoelastic linear region, the applied strain was controlled at 5%. The thermal stability of the samples during rheological testing was checked by a time sweep, where the parent polymers gave a stable G' at over 20 min at 200°C, and all of the tests were completed within 13 min.

DSC

The thermal properties of the blends were analyzed with a TA Instruments, New Castle, Delaware DSC Q20 with samples of about 5–7 mg sliced from the extruded pellets. Experiments were carried out under dry nitrogen. The samples were heated to 160°C rapidly, held at 160°C for 5 min, and then cooled to 40°C at a rate of 10°C/min. They were then heated from 40 to 160°C at a rate of 10°C/min. The second heating scan was recorded and analyzed. Calculations of crystallinity were based on a heat of fusion of 290 J/g for the ideal PE crystal.[24]

Mechanical testing

The mechanical properties were tested on an AGS-J universal testing machine (Shimadzu Co., Ltd., Kyoto, Japan), and the crosshead speed was 100 mm/min. The testing was performed at 23°C, and the geometry of the specimens, number of specimens, test conditions, procedure, and calculations were according to ASTM D 638. The notched impact test was performed on a UJ-40 (Hebei Chengde Material Testing Machine factory, Chengde, PR China) impact tester at room temperature according to ASTM D 256.

RESULTS AND DISCUSSION

Rheological properties

The rheological data given in this article were obtained at 180°C, except for those with special explanation.

The dependence of G' and G'' on the frequency at 180°C for all of the samples is shown in Figure 1. G' translates the elastic behavior of the material and is related to the amount of stored energy, whereas G'' represents the amount of dissipative energy. Figure 1(a) shows that HMW possessed the highest value of G', whereas LMW possessed the lowest value, because HMW had a higher M_w; this plays an important role in the elasticity. The larger M_w is, the higher G' will be. The G' value of the blends increased gradually with increasing fraction of HMW, and the G'' of value of the system showed the same trend with G', as shown in Figure 1(b). With increasing M_w, much more energy is needed to be dissipated because of the motion of polymer chains, which results in a higher G''. It was also found that all of the values of the slopes of the plots of log G' versus log ω (where ω is the angular frequency) and log G'' versus log ω were lower than those of a monodisperse polymer system (namely, 2 for log G' vs log ω and 1 for log G'' vs log ω, according to the linear viscoelastic theory) because of the polydispersity of the system.

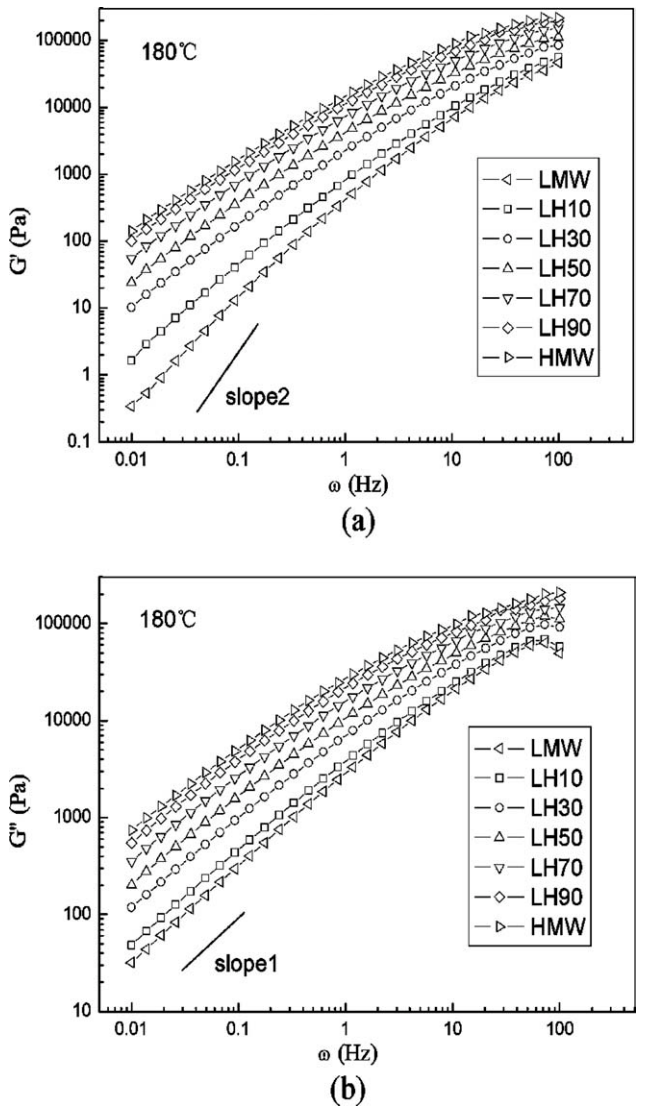

Figure 1 Modulus versus frequency for LMW/HMW blends at 180°C: (a) G' and (b) G''.

Figure 2 shows the complex viscosity (η*) curves of the LMW/HMW blends. LMW showed a zero shear viscosity (η^0) plateau that expanded over 2 decades and showed quite weak shear thinning over the whole range of ω studied. For the systems studied, LMW exhibited the lowest η* because of its low M_w, and the η* of the LMW/HMW blends was found to lie between the pure components over the whole range of ω studied. A gradual increase in η* was observed with increasing HMW content, which suggested the miscibility of the components in the blends.[32]

In this study, the additivity rule was used to calculate M_w of the blends with M_w values of the parent components. The calculated results are collected in Table I. It was reported that the additivity rule was valid for M_w of PE blends, and the calculated and measured M_w values fit quite well with each other according to Krumme et al.[40]

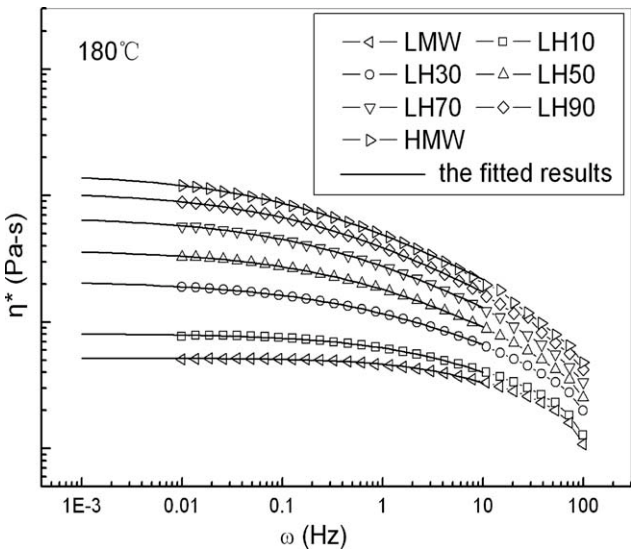

Figure 2 η* versus ω for LMW/HMW blends at 180°C.

The Cross model was used to fit η* to obtain η^0, and as shown in Figure 2, this model gave a reasonably good fit to our experimental data:

$$\eta^* = \eta^0/[(1 + \tau_0\omega)^{1-n})] \quad (1)$$

where, τ_0 is the characteristic time, and 1−n is the rate index. The fitted values of η^0 are presented in Table I.

Figure 3 shows the η^0 of the blends as a function of M_w. The dependence of η^0 on M_w is usually expressed by the well-known power law:

$$\eta^0 = K \times M^a$$

where M is the weight average molecular weight, K is a coefficient depending on polymer materials and the test temperature, exponent a is 3.2–3.6 for

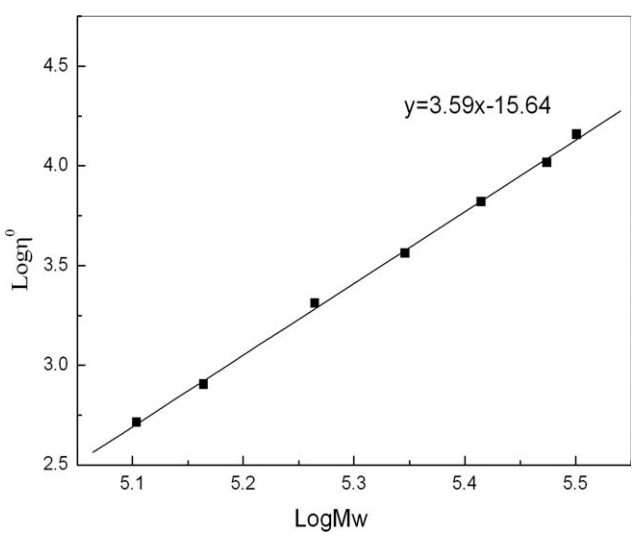

Figure 3 Correlation between η^0 and M_w of the blends.

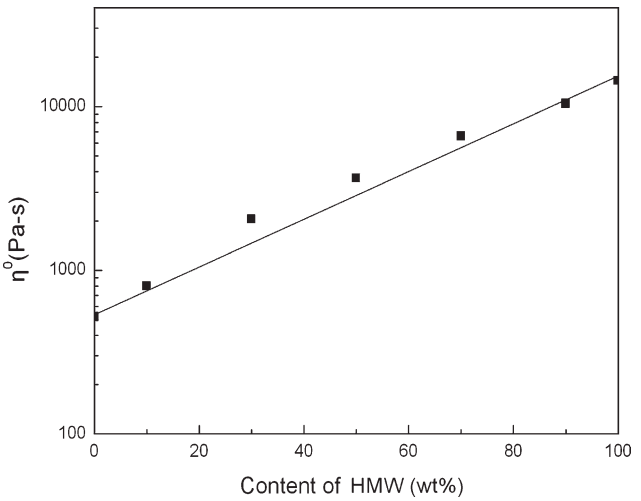

Figure 4 η^0 as a function of the blend composition for the blends.

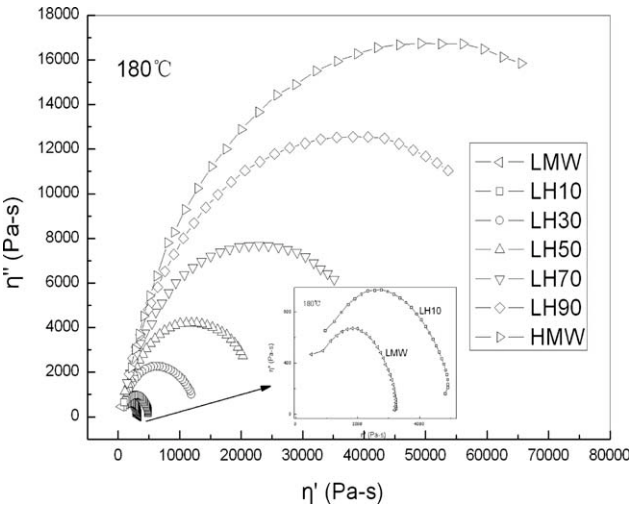

Figure 5 Cole–Cole plot for the blends: η'' versus η'.

conventional PEs[41] and the data in Figure 3 fit to a straight line ($\eta^0 = K \times M^{3.59}$). η^0 (wt %) values for the blends are plotted in Figure 4, and the increase in η^0 for all of the blend compositions was found to follow the increase in the fraction of the more viscous component, HMW. In addition, η^0 (wt %) values for the blends were found to approximately follow the logarithm of additivity, which also suggested that the components in the blends were miscible.[42] η^0 was obtained from model calculation. Therefore, the small deviations of η^0 from the logarithm of additivity were ignored.

Cole–Cole plots, consisting of the imaginary viscosity (η'') versus real viscosity (η') plot,[7] were also used to analyze the rheological data. Although it is an empirical method, it has been widely used to analyze the miscibility of polymer blends. If the blend was miscible, the curve would form a semicircular shape, and a smooth, semicircular shape suggests good miscibility. The Cole–Cole plots of the blends are shown in Figure 5, and the results display plots with semicircular shapes, with all of the data for the blends lying between those of the pure components. Again, this result suggests the miscibility of the LMW/HMW blends, regardless of the blend compositions. Hence, the Cole–Cole plots supported the previous results of η^0 (wt %).

Han plots, presented as curves of G' versus G'' in logarithmic scale proposed by Han et al.,[43] were also adopted to judge the miscibility of the polymer blends. For a homogeneous polymer system, the Han curve is not dependent on either the temperature or the composition.[43] Han plots of the blend system are presented in Figure 6. The data did not fit well to a single correlation for all of the compositions. The values of the slopes and the regression coefficient (R^2) of the linear fitted curves are listed in Table II. Han and Kim[44] proposed that in the linear region, where $0 < \omega\tau_d \approx 1$ (τ_d is the tube disengagement time) of flexible, entangled polydisperse polymers

$$\log G' = x \log G'' + (1 - x) \log(8G_N^0/\pi^2)$$

where G_N^0 is the plateau modulus $1 < x < 2$. This indicates that the slope of log G' versus log G'', was less than 2. Both slopes of the two parent polymers were less than 2 because of the polydispersity of the molecular weight. Even the two parent polymers were different in slope. This means that the classical independence of the Han plot on the composition could not be used to judge the miscibility of the studied blend system. However, all of the slopes for the blends were between the two parent polymers. This suggested miscibility, consistent with the previous analysis. A Han plot for every blend system was

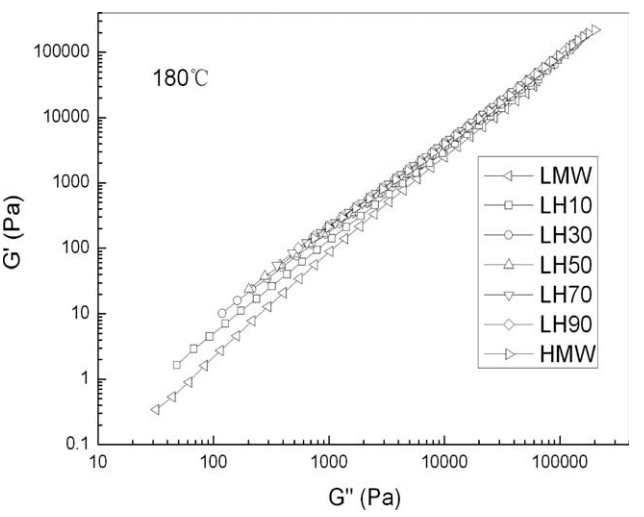

Figure 6 Han curves, G' versus G'' in logical scale for the blends.

TABLE II
Slopes and R^2 Values of the Han Plots

Sample	LMW	LH10	LH30	LH50	LH70	LH90	HMW
Slope	1.5	1.38	1.32	1.31	1.31	1.31	1.31
R^2	0.9995	0.9999	0.9999	0.9999	0.9999	0.9998	0.9997

also obtained at different temperatures, namely, 140, 160, 180, and 200°C. The results of LH50 are presented in Figure 7, whereas Han plots of the others are not shown because every blend had the same trend as LH50. The plots were independent of temperature, which indicated the thermorheological simplicity in melt state.

To certificate the thermorheological simplicity of the blends in melt state, the time–temperature superposition (TTS) principle was introduced. The dynamical rheological frequency sweeps of all of the LMW/HMW blends were carried out at different temperatures, namely, 140, 160, 180, and 200°C. Figure 8 shows the master curves of G' and G'' as functions of the shifted frequency ($\alpha_T\omega$) for LH50 at the reference temperature of 140°C. The master curves of other blends are not given because they showed the same trend as LH50. As shown in Figure 8, the TTS principle worked well, and excellent superposition for both G' and G'' was obtained. This suggested the thermorheological simplicity, in accordance with the results of the Han curves. By combining these results with the previous rheological results, we confirmed the miscibility of the LMW/HMW blends in the melt state.

Thermal analysis

The curves of the DSC melting scans of the samples are plotted in Figure 9. All of the blends showed a single melting peak with T_m decreasing with the addition of HMW; this indicated the miscibility of these blends. However, the two pure components presented a single melting peak and had little difference in the melting temperature. Even if the two components formed their own peaks for the blends during the period, they may have been covered up by each other. Then, only one peak could be seen. Whether crystallization will result in phase separation and influence the mechanical properties is discussed later. Figure 10 shows the crystallinity of the blends versus the blend composition, and the crystallinity approximately followed the linear additivity with the content of HMW.

Mechanical properties

Figure 11 depicts the notched impact strength as a function of HMW content, and the impact strengths of LMW and HMW were 4.5 and 29.7 kJ/m^2, respectively. The impact strength of HMW was much higher than that of LMW, and those of the blends were lower than that calculated by the rule of mixture. A large negative deviation from linear additivity suggested the incompatibility of these blends in the solid state.

Figure 12 shows the tensile yield strength and elongation at break of LMW, HMW, and the blends. LMW showed the highest tensile yield strength, whereas HMW showed the lowest because of the higher crystallinity of LMW. The tensile yield strength of the blends was found to be in accordance

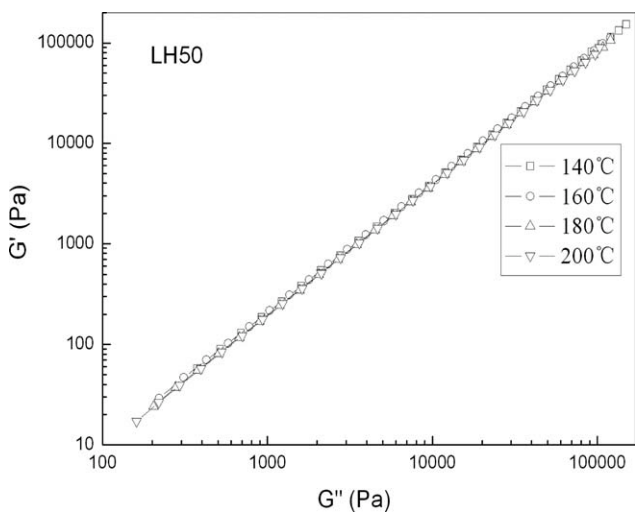

Figure 7 Han curves for LH50 at different temperature.

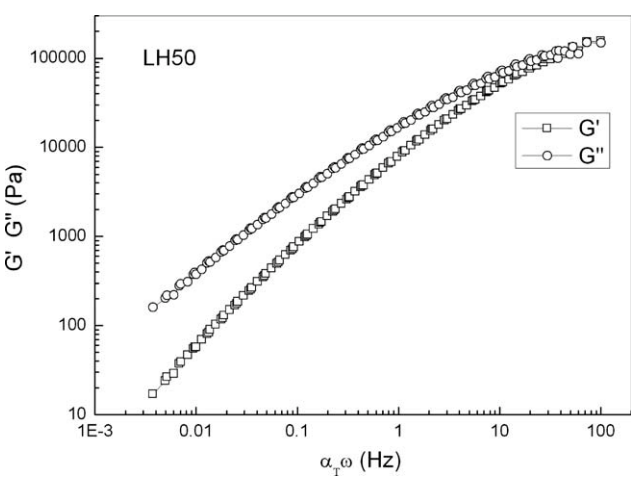

Figure 8 Master curves of LH50 at the reference temperature of 140°C.

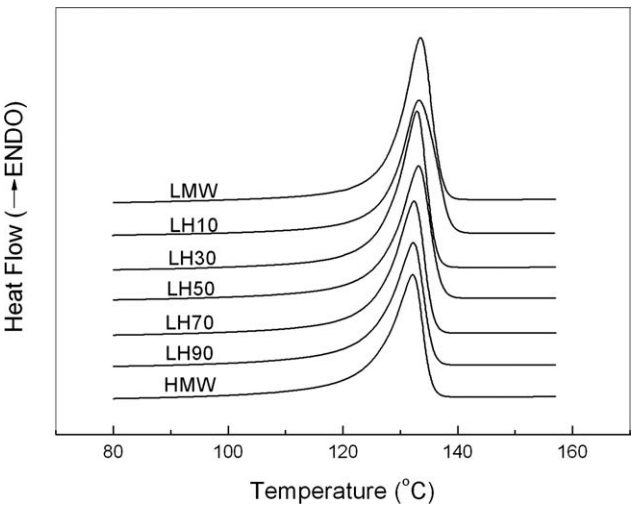

Figure 9 DSC heating scans for LMW/HMW blends.

with the linear additivity. LMW broke at the lowest elongation, whereas HMW did not break, even at an elongation of 1000%. The blends showed negative deviation from the linear additivity results of the pure resins. This seemed to contradict with the trend of the tensile yield strength. Actually, the tensile properties measured at a low strain level were a function of crystallinity, whereas the properties measured at a high strain level were determined by the extent of the compatibiliy.[45] Thus, the tensile yield strength, which was measured at low strain, showed the same phenomena as the crystallinity, discussed previously, and followed the linear additivity rule, whereas the elongation at break showed negative deviation, which was measured at a high strain; this suggested the incompatibility of the blends.

The rheological results of the melt miscibility and the mechanical properties seemed to be inconsistent. The melt rheology suggested miscibility, whereas

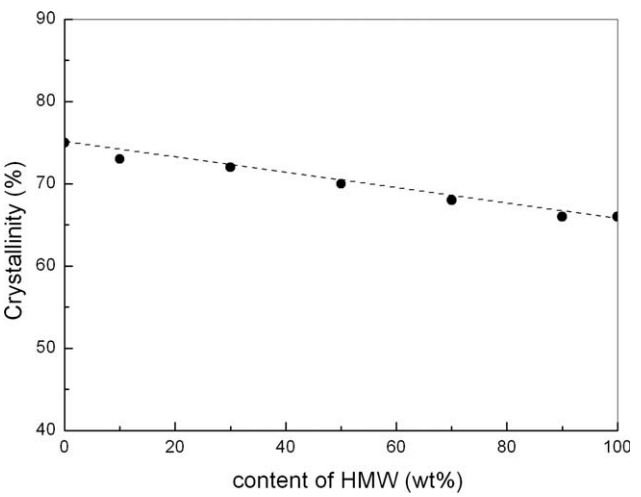

Figure 10 Percentage crystallinity as a function of composition for LMW/HMW blends.

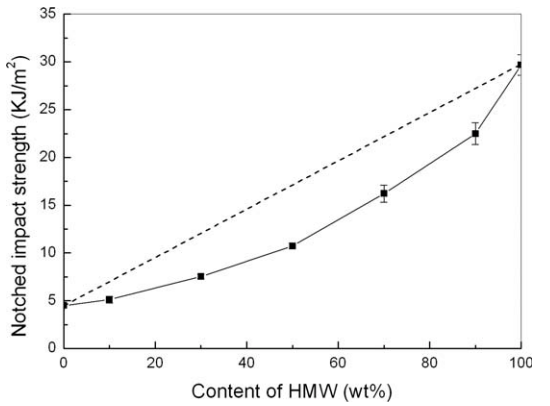

Figure 11 Impact strength of the blends plotted as a function of blend composition.

the mechanical properties indicated some sort of incompatibility. However, the rheology data were obtained in the melt state, and the mechanical properties data were obtained in the solid state. The incompatibility of the PE blends in the solid state may have resulted from the phase separation of the components in the course of cooling to room temperature, in which the crystallization occurred. So, the miscibility in the melt state did not always result in the good compatibility shown in the solid state. Krumme et al.[40,46] assumed that both M_w and short-chain branch had an effect on the crystallization behavior of HDPE blends but that the effect of M_w was the dominating parameter. Further studies in our research should concentrate on the details of crystallization-induced phase separation, which will be beneficial for us to control and tailor the structure and properties of PE blends.

CONCLUSIONS

The rheological and mechanical properties of blend systems of two HDPEs with different M_w values

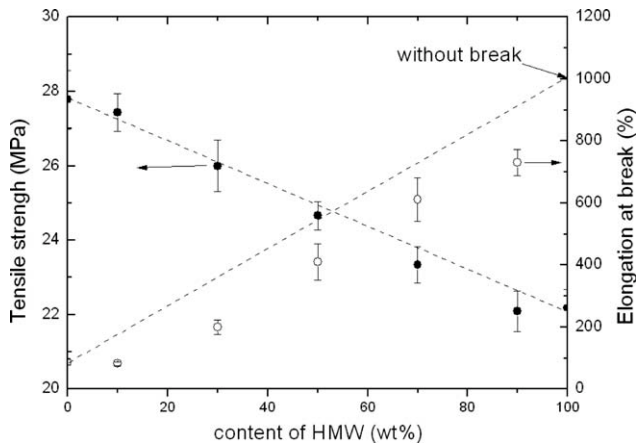

Figure 12 Tensile strength and elongation at break of the blends plotted as a function of blend composition.

were studied. The rheological measurements results showed that the rheological behavior of the blends departed from the classical linear viscoelastic theory because of the polydispersity of the HDPEs that we used. The plots of the log η^0 versus the blend composition, Cole–Cole plots, Han curves, and master curves of G' and G'' confirmed that the LMW/HMW blends were miscible in the melt state. The tensile yield strength, which was insensitive to the phase segregation, generally followed linear additivity, whereas the elongation at break and impact strength results were lower than that predicted by linear additivity and suggested the incompatibility of the blends in the solid state. The results suggest that some changes occurred during the liquid–solid transformation, and more work should be done to elucidate the phase separation during the cooling or crystallization of the blends from the miscible melt state.

References

1. Utracki, L. A. Polymer Alloys and Blends: Thermodynamics and Rheology; Hanser: New York, 1989.
2. Fang, Y.; Carreau, P. J.; Lafleur, P. G. Polym Eng Sci 2005, 45, 1254.
3. Micic, P.; Bhattacharya, S. N.; Field, G. Int Polym Proc 1996, 11, 14.
4. Husssein, I. A.; Williams, M. C. Polym Eng Sci 2001, 41, 696.
5. Rana, D.; Lee, C. H.; Cho, K.; Lee, B. H.; Choe, S. J Appl Polym Sci 1998, 69, 2441.
6. La Mantia, F. P.; Valenza, A.; Acierno, D. Eur Polym J 1986, 22, 647.
7. Cho, K.; Lee, B. H.; Hwang, K. M.; Lee, H.; Choe, S. Polym Eng Sci 1998, 38, 1969.
8. Nesarikar, A.; Crist, B.; Davidovich, A. J Polym Sci Part B: Polym Phys 1994, 32, 641.
9. Hill, M. J.; Barham, P. J. Polymer 1997, 38, 5595.
10. Alamo, R. G.; Londono, J. D.; Mandelkern, L. F.; Stehling, C. G.; Wignal, D. Macromolecules 1994, 27, 411.
11. Barham, P. J.; Hill, M. J.; Keller, A.; Rosney, C. C. A. J Mater Sci Lett 1988, 7, 1271.
12. Hill, M. J.; Barham, P. J.; Keller, A.; Rosney, C. C. A. Polymer 1991, 32, 1384.
13. Hill, M. J.; Barham, P. J.; Keller, A. Polymer 1992, 33, 2530.
14. Hill, M. J.; Barham, P. J. Polymer 1992, 33, 4099.
15. Hill, M. J.; Barham, P. J. Polymer 1992, 33, 4891.
16. Hill, M. J.; Barham, P. J.; van Ruiten, J. Polymer 1993, 34, 2975.
17. Puig, C. C.; Hill, M. J.; Barham, P. J. Polymer 1993, 34, 117.
18. Alamo, R. G.; Londono, J. D.; Mandelkern, L.; Stehling, F. C.; Wignal, G. D. Macromolecules 1994, 27, 411.
19. Alamo, R. G.; Graessley, W. W.; Krishmamoorti, R.; Lohse, D. J.; Londono, J. D.; Mandelkern, L.; Stehling, F. C.; Wignal, G. D. Macromolecules 1997, 30, 561.
20. Tanem, B. S.; Stori, A. Polymer 2001, 42, 4309.
21. Hill, M. J.; Barham, P. J. Polymer 1995, 36, 1523.
22. Utracki, L. A. Polymer Alloys and Blends; Hanser: New York, 1989; p 131.
23. Hussein, I. A. Polym Int 2004, 53, 1327.
24. Hussein, I. A. Polym Int 2005, 54, 1330.
25. Hussein, I A.; Hameed, T. J Appl Polym Sci 2005, 97, 2488.
26. Hussein, I. A. Macromolecules 2003, 36, 2024.
27. Hameed, T.; Hussein, I. A. Polymer 2002, 43, 6911.
28. Hussein, I. A.; Hameed, T.; Abu-Sharkh, B. F.; Mezghani, K. Polymer 2003, 44, 4665.
29. Hameed, T.; Hussein, I. A. Macromol Mater Eng 2004, 289, 198.
30. Hussein, I. A.; Williams, M. C. Rheol Acta 2004, 43, 602.
31. Hussein, I. A.; Williams, M. C. Polym Eng Sci 2004, 44, 660.
32. Hameed, T.; Hussein, I. A. Polym J 2006, 38, 1114.
33. Fang, Y.; Carreau, P. J.; Lafleur, P. G. Polym Eng Sci 2005, 45, 1254.
34. Lee, H.; Cho, K.; Ahn, T. K. J Polym Sci Part B: Polym Phys 1997, 35, 1633.
35. Kwag, H.; Rena, D.; Cho, K. Polym Eng Sci 2000, 40, 1672.
36. Munoz-Escalona, A.; Lafuente, P.; Vega, J. F.; Munoz, M. E.; Santamaria, A. Polymer 1997, 38, 589.
37. Krishnaswamy, R. K.; Yang, Q. Polymer 2007, 48, 5348.
38. Bai, L.; Li, Y. M.; Yang, W.; Yang, M. B. Polym Mater Sci Eng, 2010, 26, 103.
39. Utracki, L. A.; Schlund, B. Polym Eng Sci 1987, 27, 359.
40. Krumme, A.; Lehtinen, A.; Viikna, A. Eur Polym J 2004, 40, 359.
41. Vega, J. F.; Munoz-Escalona, A.; Santamarıa, A.; Munoz, M.; Lafuente; E. P. Macromolecules 1996, 29, 960.
42. Liu, C. Y.; Wang, J.; He, J. S. Polymer 2002, 43, 3811.
43. Han, C. D.; Lem, K. W. Polym Eng Rev 1982, 2, 135.
44. Han, C. D.; Kim, J. K. Polymer 1993, 34, 2533.
45. Jose, S.; Aprem, A. S.; Francis, B. Eur Polym J 2004, 40, 2105.
46. Krumme, A.; Lehtinen, A.; Viikna, A. Eur Polym J 2004, 40, 371.